Available online at www.sciencedirect.com
SCIENCE DIRECT®
ELSEVIER
Earth and Planetary Science Letters 212 (2003) 457–470
EPSL
www.elsevier.com/locate/epsl

The effect of dissolved magnesium on diffusion creep in calcite

Marco Herwegh *, Xiaohui Xiao, Brian Evans

Department of Earth, Atmospheric, and Planetary Sciences, Massachusetts Institute of Technology, Cambridge, MA 02139, USA

Received 5 December 2002; received in revised form 13 May 2003; accepted 14 May 2003

Abstract

We experimentally tested a series of synthetic calcite marbles with varying amounts of dissolved magnesium in a standard triaxial deformation machine at 300 MPa confining pressure, temperatures between 700 and 850°C, stresses between 2 and 100 MPa, and strain rates between 10^{-7} and 10^{-3} s^{-1}. The samples were fabricated by hot isostatic pressing of a mixture of calcite and dolomite at 850°C and 300 MPa. The fabrication protocol resulted in a homogeneous, fine-grained high-magnesian calcite aggregate with minimal porosity and with magnesium contents between 0.07 and 0.17 mol% $MgCO_3$. At stresses below 40 MPa the samples deformed with linear viscosity that depended inversely on grain size to the 3.26 ± 0.51 power, suggesting that the mechanisms of deformation were some combination of grain boundary diffusion and grain boundary sliding. Because small grain sizes tended to occur in the high-magnesium calcite, the strength also appeared to vary inversely with magnesium content. However, the strength at constant grain size does not depend on the amount of dissolved magnesium, and thus, the impurity effect seems to be indirect. At stresses higher than 40 MPa, the aggregates become non-linearly viscous, a regime we interpret to be dislocation creep. The transition between the two regimes depends on grain size, as expected. The activation energy for diffusion creep is 200 ± 30 kJ/mol and is quite similar to previous measurements in natural and synthetic marbles deformed at similar conditions with no added magnesium.

Keywords: calcite; diffusion creep; solid solution impurities; deformation mechanism

1. Introduction

Calcite rocks are important crustal rocks that often take up intensive deformation, the style of which may be either penetrative or localized [1–7]. Consequently, deformation in carbonates is an important topic in understanding tectonic processes and orogenic events.

Depending on stress, strain rate, and grain size, the deformation of calcite rocks at elevated temperature and low strain rates is dominated either by linear viscous creep involving the motion of point defects and grain boundary sliding or by dislocation creep involving dislocation migration

* Corresponding author. Present address: Institut für Geologie, Universität Bern, CH-3012 Bern, Switzerland. Tel.: +41-31-631-8764; Fax: +41-31-631-4843.
E-mail addresses: marco.herwegh@geo.unibe.ch (M. Herwegh), xhxiao@mit.edu (X. Xiao), brievans@mit.edu (B. Evans).

0012-821X/03/$ – see front matter © 2003 Elsevier Science B.V. All rights reserved.
doi:10.1016/S0012-821X(03)00284-X

[8–13]. The strain rate ($\dot{\varepsilon}$) in the diffusion and dislocation creep regimes is often described by a constitutive equation of the form:

$$\dot{\varepsilon} = \dot{\varepsilon}_0 \frac{\sigma^n}{d^m} \exp(-Q/RT) \quad (1)$$

where $\dot{\varepsilon}_0$ is a pre-exponential factor that may contain terms dependent on fugacity or those weakly dependent on temperature, σ is the differential stress, Q is the activation energy, R is the gas constant, T is the absolute temperature, n is a constant often called the stress exponent, and m is the sensitivity of strain rate to grain size (d). Theoretical models of linear viscous creep controlled by diffusion processes require $n=1$ and $m=2$ (Nabarro–Herring creep) or $m=3$ (Coble creep). In this contribution, for the sake of brevity, we call this deformation diffusion creep without intending to imply that deformation is controlled by diffusion or grain boundary sliding [13–15].

Although some workers have questioned the application of Eq. 1 to dislocation creep in calcite rocks [8,16,17], when Eq. 1 is applied, n values are usually determined to be between 3 and 9 [12,18,19]. Specific fields in temperature–stress space are attributed to diffusion and dislocation creep as the two end-member mechanisms [20,21]. In the region of transition between the two, both mechanisms are active [22], and n is found to be between 2 and 5 [13]. Interestingly, extrapolations of the constitutive rate equations for quartz and calcite (Eq. 1) to natural conditions indicate that, at intermediate metamorphic grade, grain-size-sensitive flow (diffusion creep) will dominate deformation of calcite rocks if the grain size is less than 1 mm [18].

Natural calcite typically contains divalent impurity cations including, for example, Fe, Mg, Mn, and Sr [1]. In this context it is important to note that many limestones originally were composed of aragonite and high-Mg calcite, which were then replaced by low-Mg calcite during diagenesis. As a consequence Mg nowadays is present in most natural limestones of marine origin. Furthermore, the Ca–Mg solid solution system is of special interest because the two end-member minerals, calcite ($CaCO_3$) and dolomite ($CaMg(CO_3)_2$), are commonly associated and because the mutual exchange of Mg and Ca is used as a geothermometer [23]. Although numerous deformation experiments have been performed on relatively pure calcite aggregates at high temperature [10–13], few experimental data exist for the rheological behavior of calcite with systematically varied chemical impurity content. Wang et al. [24] and Freund et al. [25] have performed creep tests on calcites with trace amounts of Mn (20–600 ppm). Those authors suggested that for diffusion creep of polycrystals, and, under some conditions, for dislocation creep of single crystals, the solid solution of Mn may affect the creep rate of the calcite solvent. For diffusion creep, this behavior is attributed to enhanced grain boundary diffusivity, while for dislocation creep the Mn–Ca exchange may affect the neutrality conditions and point defect concentrations. No such data exist for Mg solid solutions, notwithstanding the importance of this cation in natural limestones.

This study particularly focuses on the influence of Mg solute on diffusion creep in Mg-calcite. We produced a set of synthetic calcite aggregates with varying amounts of dissolved Mg and then subjected them to conventional triaxial mechanical tests in a gas-medium deformation apparatus.

2. Methodology of experiments

Samples were prepared and tested in three steps: (1) mixing and forming of powders (in ceramics processing, this step is often called green body preparation); (2) densification and homogenization of the high-magnesian calcite polycrystals at elevated pressures and temperatures (hot isostatic pressing or HIP [26,27]); and (3) mechanical testing in a conventional triaxial configuration [28]. An extensive suite of HIP experiments was run to determine the conditions that were necessary to complete the solid solution reaction. Generally all dolomite was dissolved in the experiments, except for few runs (Mgcc-80, see below), which were designed to have a final Mg-calcite composition located exactly on the calcite solvus (Fig. 1). In addition, there might be some small

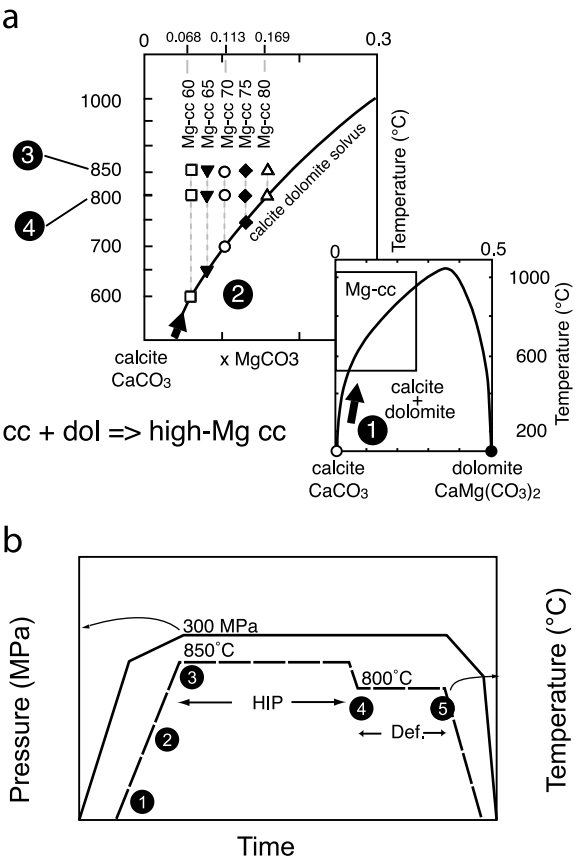

Fig. 1. Chemistry and conditions for the HIP phase. (a) Phase diagram for the system calcite–dolomite (after [23]). The numerical labels enclosed in filled circles are as follows: 1: complete phase diagram; 2: partial phase diagram with compositions of the calcite–dolomite mixtures (in molar fractions). Solution occurs as the samples are heated and the mixtures cross the calcite–dolomite solvus; 3: HIPing condition for all the mixtures; 4: temperature during creep tests. (b) Pressure (solid line) and temperature (dashed line) versus time. Number labels 1–4 are the same as in panel a. Label 5 shows the time at the beginning of quenching.

inhomogeneity in solid solution concentrations. For creep tests, the Fe jackets were filled with a single calcite–dolomite green body, HIPed (see below), and then deformed without removing the densified and homogenized aggregate.

2.1. Powder preparation

The starting powders were natural dolomite (Microdol Super from Alberto Luisoni Mineralstoffe) and reagent-grade calcite (Mallinckrodt). The dolomite powder was milled in a mechanical mortar and pestle for several hours, resulting in an average grain size of about 2 μm. The starting grain size of calcite was around 10 μm, and this powder was used as received. The final $MgCO_3$ content of the calcite was pre-defined by mixing the appropriate proportions of calcite and dolomite (see Table 1 and points 1 and 2 in Fig. 1a,b) in the mortar and pestle.

Each of the mixed powders was dried in an oven overnight at 110°C, and cold-pressed into an iron shell to form a green body. The ends of the shells were covered by Al_2O_3 spacers (length 3 mm), Al_2O_3 pistons (length 50 mm) and ZrO_2 cylinders (length 30 mm) (Fig. 2). In order to quantify the grain sizes of Mg-calcites after HIP, but prior to deformation, a series of experiments were run with samples composed of equal aliquots of five different calcite–dolomite mixtures, cold-

pressed into green bodies, and then placed in a single iron shell. Al_2O_3 spacers (1.5 mm) separated the individual batches from each other.

2.2. Hot isostatic pressing

The whole assembly was mounted into an iron jacket (Fig. 2) and then pressurized to 225 MPa in a gas-medium deformation apparatus (Paterson Instruments/ANU Tech). In order to reduce sample humidity and porosity, a rough vacuum was simultaneously applied to the pore pressure vent. The vacuum pump was then turned off and the furnace heated at 15°C/min to 850°C. Once the experimental conditions were reached, the specimen was HIPed at constant temperature and 300 MPa for 0–18 h (Table 1, point 3 in Fig. 1a,b). Before each set of experiments, a furnace calibration and adjustment guaranteed a homogeneous temperature profile across the sample area. During the experiment the temperature was monitored by three Pt–Pt/Rh thermocouples internal to the furnace and an additional chromel–alumel thermocouple placed on top of the sample. The temperature variability, both temporal and spatial, was less than ±5°C.

Although the sample is initially vented during pressurization and the initial stages of heating, it becomes sealed at high temperatures by a combination of compaction and static recrystallization. Hence, an internal CO_2 pressure will build up, guaranteeing the stability of the Mg-calcite.

2.3. Creep tests

Creep tests were performed directly on the HIPed samples, i.e., without removal of the sample from the set-up, by decreasing the temperature to 800°C with 15°C/min and then equilibrating for 20 min (point 4 in Fig. 1a,b). Most of the data were obtained with stress steps. Several different loads were used on each sample, each load being held for a small incremental strain (0.1–0.5%). The accumulated total strain of the sample never exceeded 10–15%, preventing artifacts induced by inhomogeneous deformation related to sample barreling. Strain rates were calculated for each stress step and were between 10^{-7} and 10^{-3} s^{-1}.

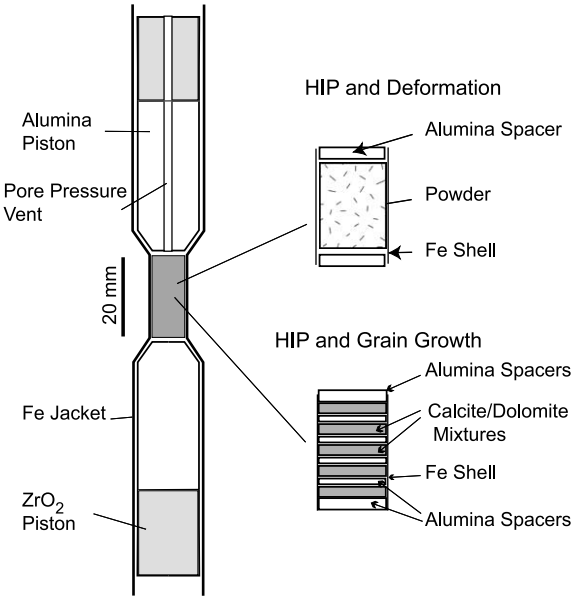

Fig. 2. Schematic cross-section of the sample assembly showing two different sample assemblies used for the deformation experiments (upper assembly) and the grain growth experiments. For the grain growth experiments, wafers with different magnesium content were stacked with alumina spacers to maximize data collection. The overall sample dimensions for both assemblies was approximately 10 mm by 20 mm.

The total time for the creep tests did not exceed 1.5–2 h per sample.

In order to obtain activation energies, for each composition an additional set of samples (2 h HIP) was generated, on which creep tests were carried out at different temperatures. As a first step, 800°C was revisited to check for reliability of the mechanical data in comparison to the first test series. Then temperatures were reduced in 50°C steps, making sure that the final temperature never fell below the calcite–dolomite solvus for that particular composition. Note that for each temperature less than 800°C, four to five stress steps were carried out. We always tried to perform tests under stress conditions for which n was as close as possible to 1. Due to experimental limitations, however, it was not possible to completely avoid a slight increase in n with decreasing temperature. The n values were determined after the creep tests by calculating best fit regressions of the creep data; n values were usually in the range of 1–1.5, and they were always smaller than 1.8.

To calculate the activation energies for the different Mg-calcites, the n values obtained from the regressions were used.

The samples were quenched from high pressure and temperature conditions by simultaneously reducing the confining pressure and turning off the furnace. This resulted in an average $\Delta P/\Delta t$ and $\Delta T/\Delta t$ of 15 MPa/min and 40°/min, respectively.

2.4. Microstructure analysis

Both HIPed and deformed samples were cut parallel to the sample axis, polished and treated with a two-step etching method similar to that used by Herwegh [29]. Unlike natural calcite mylonites, however, the weak acidic concentrations used by Herwegh [29] to etch the grain boundaries were found to be too aggressive for synthetic calcite aggregates. Therefore, we applied a gentler chemo-mechanical etching, first polishing with colloidal silica and then etching with de-ionized water. The etched samples were carbon-coated and digital images were captured in electron backscatter mode in a JEOL JXA-733 Superprobe. A grain boundary map was made by segmenting the grain boundaries with the image analysis program Image SXM and some manual adjustment. These grain boundary outlines were used to measure the area of each grain. These measurements subsequently served as basis for the calculation of the radius of a circle with an equivalent area and for the determination of both the area- and number-weighted grain size distributions. The grain size classes for the first distribution are weighted by the area percentage covered in each grain size class. For the latter distribution, the number percentage of each class is used. Area weighting allows one to check for bimodal grain size distributions, which might not be recognized in the case of number-weighted distributions.

3. Results

3.1. Starting material: chemical exchange and grain growth

The original volume proportions of dolomite and calcite were chosen so that only a single phase, Mg-calcite, was stable at 800°C and so that the compositions would range between about 0.07 and 0.17 molar fraction $MgCO_3$. The temperature of transition from calcite and dolomite to Mg-calcite for the different compositions occurred at 50°C intervals between 600 and 800°C (Fig. 1). For that reason, the different Mg-calcites will be referred to as Mgcc-60, -65, ..., -80 where the numbers indicate the transition temperature (e.g., Mgcc-60: transition temperature at 600°C). Based on scanning electron microscopy (SEM)

Table 1
Parameters of the Mg-calcite HIP and creep experiments

Mg-calcite	$MgCO_3$ (mol%)	HIP experiment	Grain size (number-weighted) (μm)	Grain size (area-weighted) (μm)	HIP time (h)	Creep experiment	n ($\sigma < 40$ MPa)	n ($60 < \sigma < 100$ MPa)
Mgcc-60	0.14	CD-47	8.79	14.55	0.333	CD-77	1.01	4.65
Mgcc-60	0.14	CD-42	11.82	19.50	2	CD-38	1.17	4.82
Mgcc-65	0.18	CD-42	10.45	17.44	2	CD-46	1.1	4.03
Mgcc-70	0.23	CD-42	9.80	15.01	2	CD-56	1.18	3.54
Mgcc-70	0.23	CD-42	9.80	15.01	2	CD-80	1.18	3.54
Mgcc-75	0.28	CD-42	8.52	13.54	2	CD-41	0.86	2.72
Mgcc-80	0.34	CD-42	7.83	11.91	2	CD-37	0.81	2.64
Mgcc-60	0.14	CD-43	13.32	22.23	6	CD-53	1.59	4.87
Mgcc-70	0.23	CD-43	10.03	17.56	6	CD-62	1.35	3.48
Mgcc-80	0.34	CD-43	9.71	14.98	6	CD-45	1.15	1.81
Mgcc-60	0.14	CD-63	23.58	33.48	18	CD-50	1.09	4.54
Mgcc-70	0.23	CD-63	14.45	22.69	18	CD-51	1.12	3.02
Mgcc-80	0.34	CD-63	12.19	17.34	18	CD-49	1.01	2.02

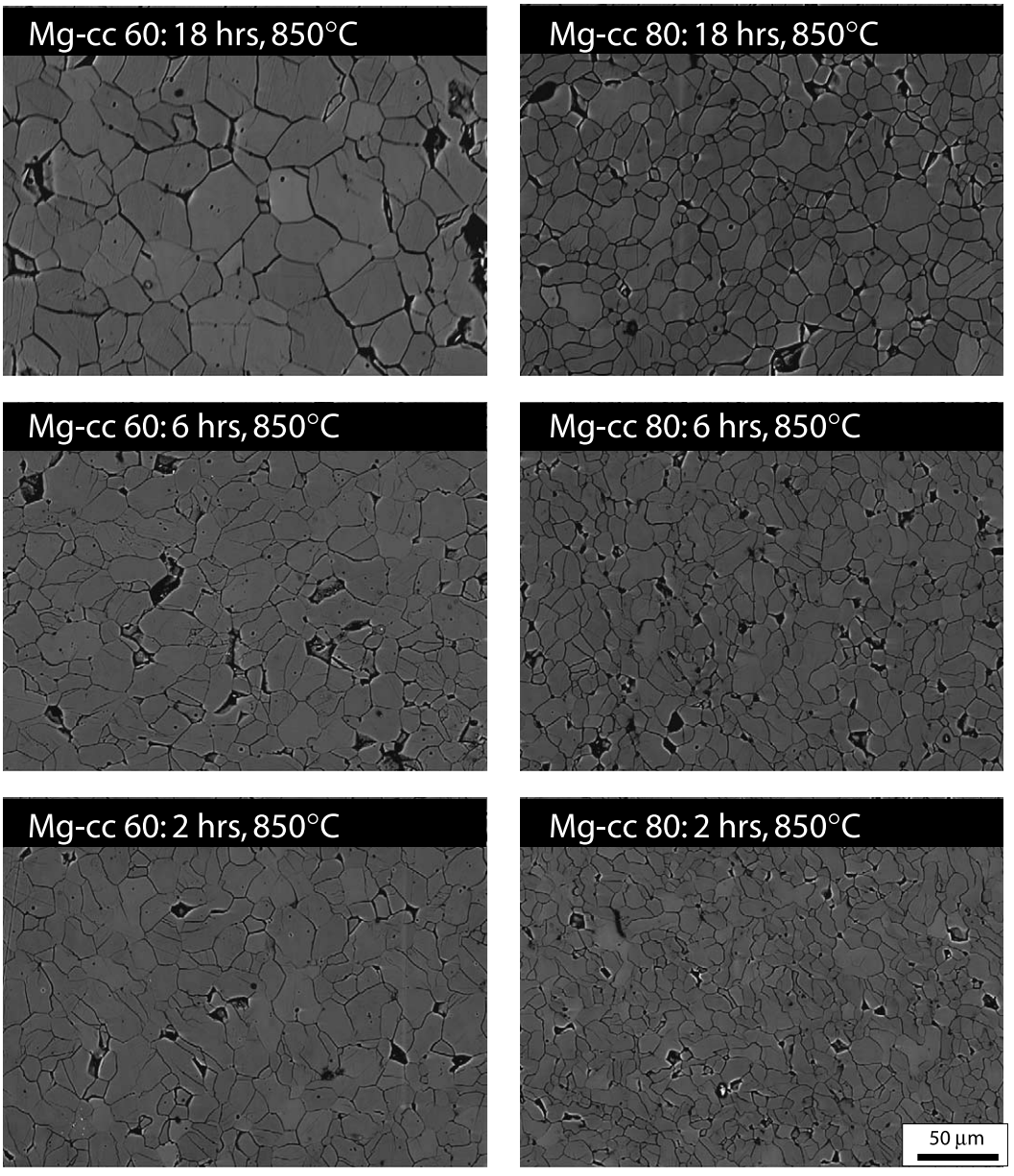

Fig. 3. Back-scattered SEM images show the microstructural evolution with increasing HIPing time for the two extreme mixtures Mgcc-60 (left column) and Mgcc-80 (right column). Scale for all the images is given in the lower right hand corner. Notice that the solid solutions with the lower magnesium content (Mgcc-60) have larger grain size at all times. Grain boundaries have been etched for emphasis. Pore spaces are probably a result of grain pull-out during polishing.

and electron microprobe observations it was established that calcite and dolomite completely transformed to Mg-calcite after HIP was completed, except in the case of the highest-Mg calcite, where less than 1% dolomite remained (Fig. 1). At this stage it should be noted that the amount of the residual dolomite was too small and the size too large to affect the entire Mg-calcite microstructure by grain boundary pinning.

The transition from original calcite and dolo-

mite to Mg-calcite is based on a complex interaction of different processes manifested by microstructural changes. After about 10 min of HIPing, for example, the grain size of the original calcite

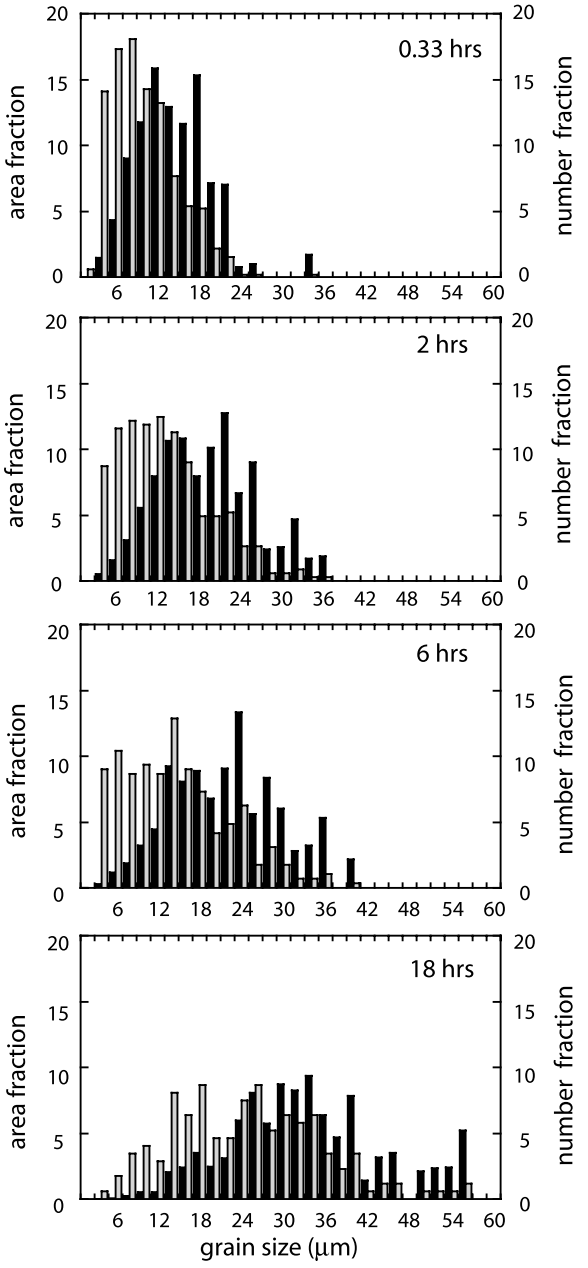

Fig. 4. Grain size evolution with increasing HIPing time for the mixture Mgcc-60. Black and gray bars represent area-weighted and number-weighted grain sizes, respectively.

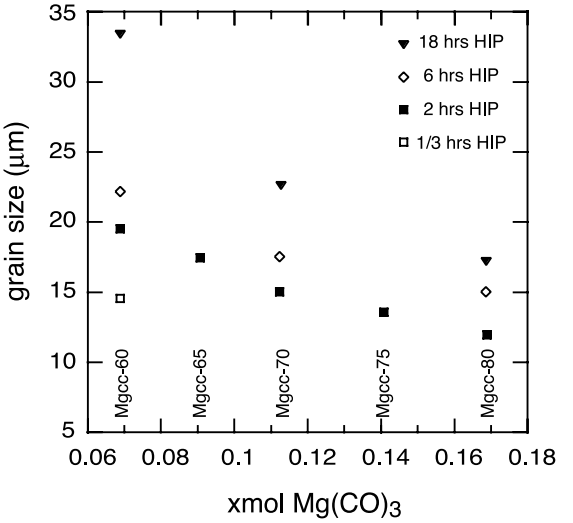

Fig. 5. Evolution of area-weighted grain size as a function of composition for several different HIPing intervals. High magnesium content correlates with smaller grain size at all intervals.

decreases owing to the onset of chemically induced grain boundary migration (CIGM). Together with diffusion processes, CIGM is the predominant process for the exchange of Ca and Mg cations between calcite and dolomite. During the transition period, several cycles of CIGM occur, each bringing the Mg content of the calcite closer to the final composition. A detailed investigation of chemical exchange behavior and grain growth kinetics is outside the scope of this paper and will be treated elsewhere (cf. [32]).

After HIP, the grains are equiaxed, with grain boundaries often meeting in 120° triple junctions; grain boundaries are slightly curved (Fig. 3). The total porosity after HIP ranged between 0.5 and 4%. The variations in porosity do not systematically correlate with the Mg content of the sample. Micrometer-sized pores occur in grain interiors, along grain boundaries, and at triple junctions. For all mixtures, the mean grain size and the ranges of grain sizes increase with HIP time ranging from 11.9 to 33.5 μm (Table 1, Figs. 3–5), but growth occurs more slowly in samples with higher magnesium content. It is therefore important to note that the grain sizes of the starting materials vary inversely with the Mg composition and di-

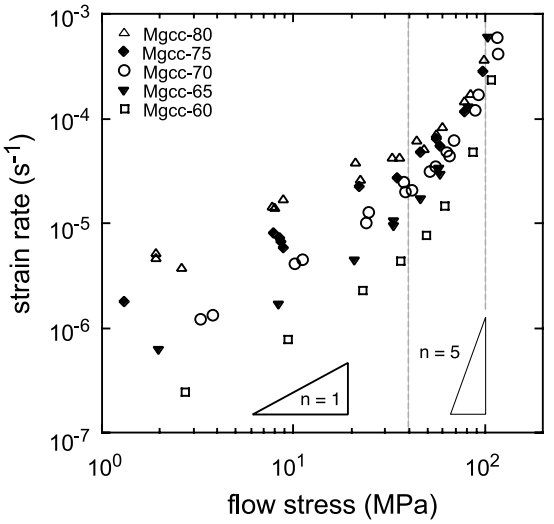

Fig. 6. Log strain rate versus log stress from creep experiments for calcites with different Mg contents (see Table 1 and Fig. 1a). All samples were deformed after 2 h HIPing. Slopes for stress exponents $n = 1$ and 5 are shown. Dashed lines indicate low-, intermediate- and high-stress regimes.

rectly with the HIP time (Fig. 5). Area-weighted distributions are symmetric Gaussian shapes, but number-weighted distributions are asymmetric (Fig. 4).

3.2. Creep tests

The relation between log stress and log strain rate for creep at 800°C of five samples with different Mg contents is shown in Fig. 6. Three distinctive regimes can be identified. (1) At low stresses (< 40 MPa) the creep curves are sub-parallel to each other [28] with n values between 0.8 and 1.1. (2) At intermediate stresses (40–100 MPa), the curves converge, with n values between 2.5 and 5. (3) At high stresses (> 100 MPa) the data fall within a narrow region. Owing to the scarcity of

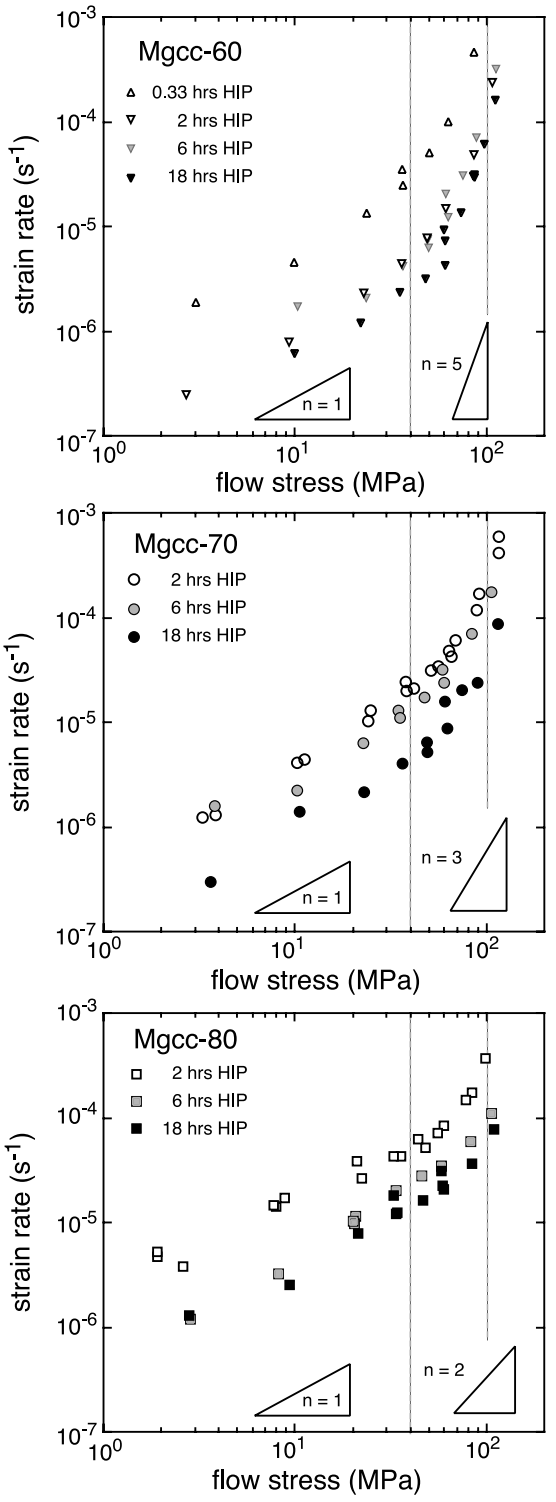

Fig. 7. Creep data for each of three Mg-calcites. Deformation experiments were begun after HIPing intervals of 0.33, 2, 6 and 18 h. For a given stress, strain rate decreases with the HIP interval used to produce the sample. Slopes of different stress exponents are shown. Dashed lines indicate low-, intermediate- and high-stress regimes.

data in the high-stress regime, n values cannot be determined accurately, but are probably greater than 4. In the low-stress regime and for a given stress, samples with higher Mg content deform with higher strain rates. Apparently, for the same stress, strain rates are faster in Mg-rich samples, while they decrease for Mg-poor ones (compare Mgcc-60–80), probably because the starting grain size also systematically covaries with Mg content (Table 1, Fig. 5).

We investigated the effect of variations in starting grain size on the creep strength by deforming samples of three different Mg contents (Mgcc-60, -70 and -80) after 2, 6 and 8 h HIP; one additional test was conducted on a Mgcc-60 sample after 0.33 h HIP (Table 1 and Fig. 7). Recall that starting grain size varies directly with HIP time. The creep data for these samples have similar characteristics at low, intermediate, and high stress. With increasing grain size, the creep curves shift towards lower strain rates. While the slopes of the creep data in the low-stress regime are subparallel to each other, the n value clearly increases with increasing stress. In the intermediate- to high-stress regimes, n increases with decreasing Mg content for a given stress.

In order to test the reproducibility between different experimental runs, we deformed two separate samples of Mgcc-70, both of which were HIPed for 2 h prior to deformation (Fig. 8a). Within experimental error, the creep curves are identical (compare scatter between them in Fig. 8). The creep data might also be influenced by changes in grain size during deformation. Fig. 8b shows two series of creep tests for Mgcc-80 (HIP 6 h) and Mgcc-70 (HIP 18 h) in which stress-stepping tests were generally made at successively higher stresses except that one or two lower stress values were revisited. The strain rates were reproducible, as long as the sample was only deformed in the low-stress regime (diffusion creep regime). For example, see steps 6–11 for sample Mgcc-70 in Fig. 8b. Note that revisiting lower stress values after deformation in the intermediate- to high-stress regime always results in higher strain rates than the original measurement (steps 8, 9 and 11 in Fig. 8b). This tendency is expected if the grain size becomes reduced due to recrystallization (e.g., subgrain rotation) in the intermediate- to high-stress regime before being tested in the diffusion creep regime. Grain size reduction during creep in the high-stress regimes on fine-grained Mn-calcites has also been reported by Freund et al. [14]. In the remainder of this study, we exclude from consideration any strength data obtained after deformation in the intermediate- to

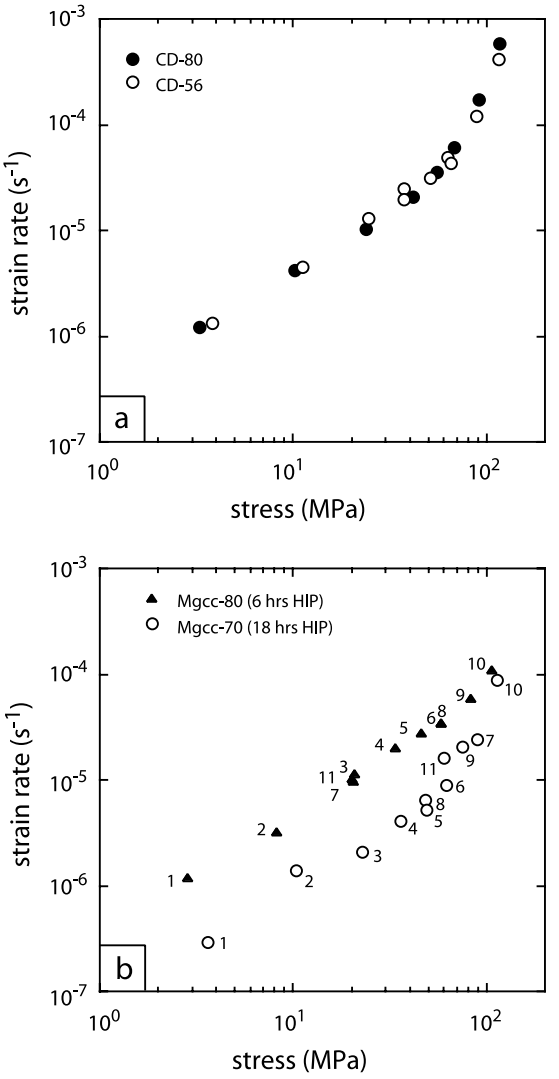

Fig. 8. Data reproducibility shown by: (a) creep data of two different samples with identical chemical composition (Mgcc-70) and HIPing time (2 h), (b) creep tests with increasing flow stresses but revisited low stress values.

high-stress regime. An additional point to be considered for deformation in the low-stress regime is the influence of syn-deformational grain growth on the stress/strain rate data. However, note that the total duration of the creep tests is considerably shorter than the HIP period for samples previously HIPed for 6 and 18 h. For kinetic reasons, syn-deformational grain growth probably does not affect rheology. Samples HIPed for only 2 h might be influenced. Because of the apparent increase in growth rates with decreasing Mg content, Mg-poor calcites might be affected the most. However, revisiting different stress conditions yields similar strain rates and the same n values even when samples differ in Mg concentration. Taken together, these facts suggest that the effect of syn-deformational grain growth on creep data can be neglected.

4. Discussion

4.1. Grain growth and magnesium content

The HIP experiments indicate that variations in Mg content directly influence grain growth kinetics of calcite. Based on observations of microstructure, we infer that transformation from calcite and dolomite to Mg-calcite occurs by a complex combination of grain boundary diffusion, volume diffusion, and chemically induced grain boundary migration. During this chemical mixing, small grains are formed along the calcite–dolomite interphase boundaries. After this initial period of reaction and mixing, normal grain growth occurs. The normal grain growth rates in these high-magnesian samples are different from that in Solnhofen limestone or in synthetic calcite marbles without added dolomite [30,31]. A detailed discussion of the mechanisms of the chemical mixing and of grain growth kinetics is outside the scope of this paper and will be treated elsewhere (cf. [32]). For the present study, it is important to notice that the grain size of these marbles is inversely correlated with Mg content, even after HIP for identical time intervals. Apparently, the high-Mg calcites grow more slowly than Mg-poor ones (Fig. 4).

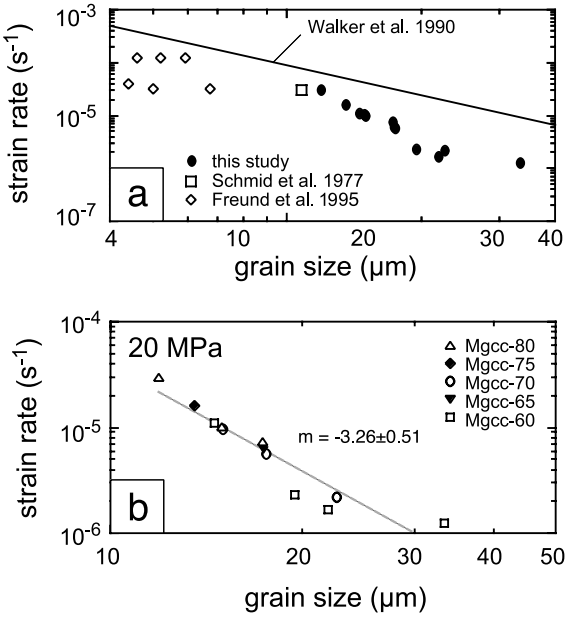

Fig. 9. Log strain rate versus log grain size for samples loaded to 20 MPa differential stress. (a) Comparison between results of the present (solid symbols) and earlier studies (open symbols). (b) Strain rate variability in terms of chemical composition. Notice that grain size, not composition, influences strain rate most strongly.

4.2. Deformation mechanisms

Descriptions of steady-state creep behavior in calcite rocks usually separate stress–strain rate space into three regimes in which strain rate shows characteristic values of sensitivity to stress and grain size, i.e., n and m, respectively [13–15,33]. At lower stresses and smaller grain sizes, changes in rheology are usually attributed to increasing importance of diffusion creep with respect to dislocation creep.

Based on the increased values of n and the decreased values of m that occur as stress increases in the range 40–100 MPa, we infer that the dominant deformation mechanism changes from diffusion creep to dislocation creep. The transition between the two occurs at higher stresses for higher Mg content and/or smaller grain size (Fig. 7), probably because diffusion creep is favored by those conditions. At higher stresses (>100 MPa), for a given Mg content, the differences in strain rate diminish for samples with differing

grain size. For a discussion of the effect of grain size during dislocation creep see also Renner and Evans [17]. In this regime, the stress exponent, n, does not seem to approach a constant value as stress increases. However, data in the dislocation creep field from our study are not extensive.

At stresses <40 MPa, $n \approx 1.1 \pm 0.2$ for all Mg contents (Figs. 6 and 7). Values of n between 1 and 2 have been observed for fine-grained calcite aggregates, both synthetic and natural (D. Freund, GFZ Potsdam, personal communication, [13,15]). The samples show inverse sensitivity of strain rate to grain size (Fig. 9), i.e., $m \approx -3.26 \pm 0.51$, similar to that observed in Mn-bearing calcites and Solnhofen limestone (Fig. 9b), but different from that observed in synthetic calcites with 1 vol% of Al_2O_3 [13], where $m \approx 1.9$. Recalling the theoretical definition mentioned in Section 1, the systematics of deformation of the high-Mg calcite samples is closer to that predicted for grain boundary diffusion (Coble creep) rather than volume diffusion.

In the diffusion creep regime, the absolute strain rate is inversely related to the Mg content and grain size, but the temperature sensitivity of log strain rate does not vary with Mg content (Fig. 10). Over the temperature interval 650–800°C, the activation energy for all the magnesian calcite samples is about 200 ± 30 kJ/mol. Similar values were obtained for diffusion creep in Solnhofen limestone (210 kJ/mol) [11,15] and at low stresses for some synthetic marbles with no added Mg (190 kJ/mol) [13].

It is less straightforward to compare the diffusion creep activation energy (200 kJ/mol) with activation energies from self-diffusion experiments performed under static conditions. Within stated uncertainty, the activation energy determined for Coble creep (200 ± 30 kJ/mol) in this study barely overlaps the activation energy for Ca grain boundary diffusion under dry conditions (267 ± 47 kJ/mol) [34] while that for O diffusion along boundaries with water present is smaller (127 ± 17 kJ/mol) [35]. Activation energies for volume diffusion in calcite vary between 170 kJ/mol (O diffusion in hydrothermal system [36] and C with dry CO_2 at 100 MPa [37]) to 382 ± 37 kJ/mol (C in dry, room pressure CO_2) [34]. Fisler and Cygan

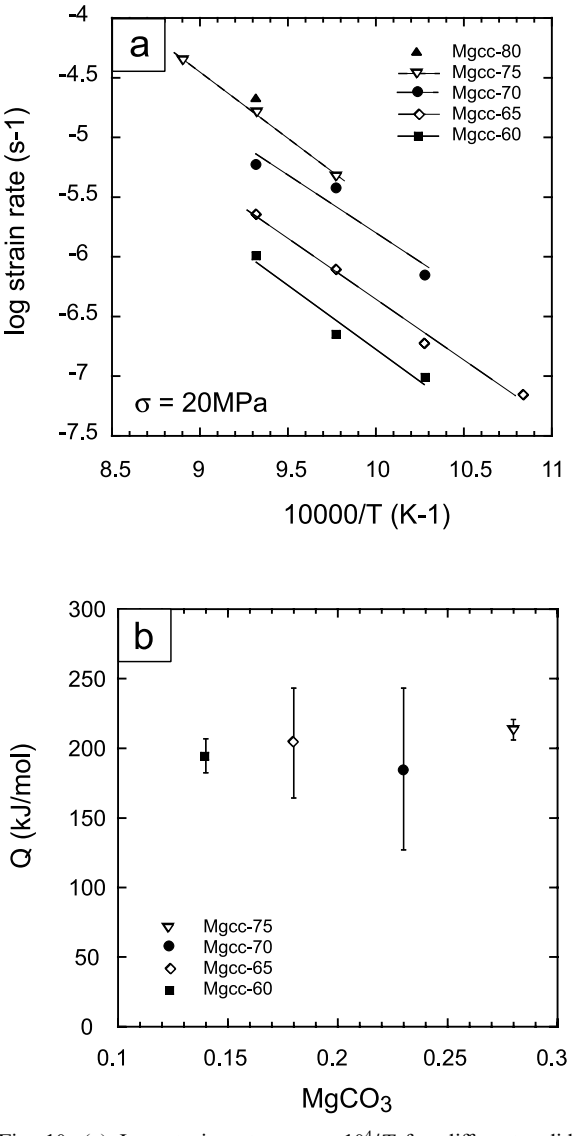

Fig. 10. (a) Log strain rate versus $10^4/T$ for different solid solutions at $\sigma = 20$ MPa. The slope is proportional to $-Q/R$ where Q is the activation enthalpy and R is the gas constant. (b) Activation enthalpy from (a) versus Mg content. Notice that, within error, the activation enthalpy does not seem to vary.

[38] showed that Ca is the slowest species for volume diffusion in the system Ca, Mg, C, O, probably because it has the largest ionic radius (see also [35,36,39]), a fact which might also be valid for the grain boundary diffusion of our experi-

ments. At present, there are few studies that constrain extrinsic effects on volume and grain boundary diffusion.

4.3. Applications

Natural carbonate rocks usually contain variable amounts of second-phase minerals, including sheet silicates, quartz or dolomite. Non-soluble second phases can suppress grain growth in a calcite matrix by boundary pinning (e.g., [31,40–42]). If solid solution is possible, dissolved magnesium could also affect grain growth kinetics and, hence, strength. Thus, variations in dolomite content within layered carbonate sediments might drastically affect calcite grain size during metamorphism. Reduction in grain size and suppression of grain growth are important aspects of strain localization and might cause deformation to be concentrated in Mg-rich layers, i.e., those layers with the smallest grain size and therefore the lowest strength (see for example fig. 13 in [1]). Such an effect might be counter-intuitive given the fact that dolomite rocks are much stronger than calcite rocks when they are deformed in the laboratory at lower temperature [43–45]. Finally, variations in grain growth kinetics can serve as an excellent tool for the design of synthetic aggregates, perhaps allowing experimenters to generate well-defined starting grain sizes.

5. Conclusions and implications

Creep experiments show that the strength of calcite aggregates correlates inversely with dissolved Mg content at stresses <40 MPa, at temperatures 700–800°C, and for small grain size. Based on the sensitivity of strain rate to stress and grain size, we posit that deformation occurs via a combination of grain boundary diffusion (Coble) creep and grain boundary sliding. The inverse correlation between strength and Mg content appears to arise from suppression of grain size with increased Mg content. That is, the effect of magnesium content on strength is indirect through an extrinsic control of calcite grain size, rather than an extrinsic control on grain boundary diffusion rate. In this diffusion creep regime, the strain rate is given by:

$$\dot{\varepsilon} = \dot{\varepsilon}_0 \frac{\sigma^{1.1}}{d^{3.26}} \exp(-Q/RT) \quad (2)$$

where the activation energy is about 200 ± 30 kJ/m, R is the gas constant, T is absolute temperature and $\dot{\varepsilon}_0$ is $4.3 \times 10^7 \pm 1.4 \times 10^7$. This activation energy is close to that in other studies where diffusion creep was measured in calcite aggregates with no added magnesium; it falls within the range of activation energies for bulk or grain boundary diffusion of Ca, C, or oxygen in calcite, but does not exactly match any current measurements.

The strength of the transition between diffusion creep and dislocation creep, as judged by increasing sensitivity of strain rate to stress, increases with decreasing grain size or increasing Mg content. Over the rather limited range of stresses explored within the dislocation creep field, the stress exponent, n, seems to increase continuously. If the same correlation between grain size and magnesium content obtains during natural deformation, calcite–dolomite mixtures may have a tendency to deform by diffusion creep if the conditions are near those necessary for the transition between the two mechanisms.

Acknowledgements

We profited from fruitful discussions with J. Renner, G. Hirth, and U. Mok and thank N. Chaterjee for help with the electron microprobe. We gratefully acknowledge Alberto Luisoni Mineralstoffe for providing the dolomite powder and financial support by the fellowship program of the Swiss National Science Foundation (SNF) (M.H.) and the U.S. National Science Foundation (NSF EAR 6892879) (B.E.). The manuscript benefited from the constructive reviews of H. De Bresser, J. Farver, S. Schmid and G. Dresen. *[SK]*

References

[1] M. Bestmann, K. Kunze, A. Matthews, Evolution of a

calcite marble shear zone complex on Thassos Island, Greece: microstructural and textural fabrics and their kinematic significance, J. Struct. Geol. 22 (2000) 1789–1807.
[2] M. Burkhard, Ductile deformation mechanisms in micritic limestones naturally deformed at low temperatures (150–350C), in: R.J. Knipe, E.H. Rutter (Eds.), Deformation Mechanisms, Rheology and Tectonics, Geol. Soc. Spec. Publ. 54 (1990) 241–257.
[3] P. Heitzmann, Calcite mylonites in the central Alpine 'root zone', Tectonophysics 135 (1987) 207–215.
[4] L.A. Kennedy, J.M. Logan, The role of veining and dissolution in the evolution of fine-grained mylonites; the McConnell Thrust, Alberta, J. Struct. Geol. 19 (1997) 785–797.
[5] L.A. Kennedy, J.M. Logan, Microstructures of cataclasites in a limestone-on-shale thrust fault; implications for low-temperature recrystallization of calcite, Tectonophysics 295 (1998) 167–186.
[6] L.A. Kennedy, J.C. White, Low-temperature recrystallization in calcite; mechanisms and consequences, Geology 29 (2001) 1027–1030.
[7] J.H.P. de Bresser, Intracrystalline deformation of calcite, Geol. Ultraiect. 79 (1991) 191 pp.
[8] J.H.P. de Bresser, C.J. Spiers, High-temperature deformation of calcite single crystals by r^+ and f^+ slip, in: R.J. Knipe, E.H. Rutter (Eds.), Deformation Mechanisms, Rheology and Tectonics, Geol. Soc. Spec. Publ. 54 (1990) 285–298.
[9] J.H.P. de Bresser, C.J. Spiers, Slip systems in calcite single crystals deformed at 300–800°C, J. Geophys. Res. 98 (1993) 6397–6409.
[10] E.H. Rutter, M. Casey, L. Burlini, Preferred crystallographic orientation development during the plastic and superplastic flow of calcite rocks, J. Struct. Geol. 16 (1994) 1431–1446.
[11] S.M. Schmid, Rheological evidence for changes in the deformation mechanism of Solnhofen limestone towards low stress, Tectonophysics 31 (1976) T21–T28.
[12] S.M. Schmid, M.S. Paterson, J.N. Boland, High temperature flow and dynamic recrystallization in Carrara marble, Tectonophysics 65 (1980) 245–280.
[13] A.N. Walker, E.H. Rutter, K.H. Brodie, Experimental study of grain-size sensitive flow of synthetic, hot pressed calcite rocks, in: R.J. Knipe, E.H. Rutter (Eds.), Deformation Mechanisms, Rheology and Tectonics, Geol. Soc. Spec. Publ. 54 (1990) 259–284.
[14] D. Freund, Z.-C. Wang, G. Dresen, High temperature creep of polycrystalline calcite: The effect of impurities (Mn), EOS Suppl. AGU Fall Meeting (1995) T51D-10, F631.
[15] S.M. Schmid, J.M. Boland, M.S. Paterson, Superplastic flow in fine-grained limestone, Tectonophysics 43 (1977) 257–291.
[16] S.J. Covey-Crump, Evolution of mechanical state in Carrara marble during deformation at 400°C to 700°C, J. Geophys. Res. 103 (1998) 29,781–29,794.
[17] J. Renner, B. Evans, Do calcite rocks obey the power-law creep equation? in: S. de Meer, M. Drury, J.H.P. de Bresser, G.M. Pennock (Eds.), Deformation Mechanisms, Rheology and Tectonics, Geol. Soc. London Spec. Publ. 200 (2002) 293–307.
[18] K.H. Brodie, R. Rutter, Deformation mechanisms and rheology: why marble is weaker than quartzite, J. Geol. Soc. 157 (2000) 1093–1096.
[19] H.P. de Bresser, B. Evans, J. Renner, On estimating the strength of calcite rocks under natural conditions, in: S. de Meer, M. Drury, J.H.P. de Bresser, G.M. Pennock (Eds.), Deformation Mechanisms, Rheology and Tectonics, Geol. Soc. London Spec. Publ. 200 (2002) 309–329.
[20] M.F. Ashby, A first report on deformation mechanism maps, Acta Metall. 29 (1982) 293–299.
[21] E.H. Rutter, Experimental study of the influence of stress, temperature, and strain on the dynamic recrystallization of Carrara marble, J. Geophys. Res. 100 (1995) 24,651–24,663.
[22] J.H.P. de Bresser, C.J. Peach, J.P.J. Reijs, C.J. Spiers, Grain size reduction by dynamic recrystallization: can it result in major rheological weakening?, Int. J. Earth Sci. (Geol. Rundsch.) 90 (2001) 28–45.
[23] L.M. Anovitz, E.J. Essene, Phase equilibria in the system $CaCO_3$-$MgCO_3$-$FeCO_3$, J. Petrol. 28 (1987) 389–414.
[24] Z-C. Wang, Q. Bai, G. Dresen, R. Wirth, B. Evans, High temperature deformation of calcite single crystals, J. Geophys. Res. 101 (1996) 20,377–20,390.
[25] D. Freund, E. Rybacki, G. Dresen, Effect of impurities on grain growth in synthetic calcite aggregates, Phys. Chem. Miner. 28 (2001) 737–745.
[26] H.J. Atkinson, B.A. Rickinson, Hot Isostatic Processing, A. Hilger, Bristol, 1991.
[27] Y. Caristan, R.J. Harpin, B. Evans, Deformation of porous aggregates of calcite and quartz using the isostatic hot-pressing technique, Tectonophysics 78 (1981) 629–650.
[28] T. Tullis, J. Tullis, Experimental rock deformation techniques, in: B.E. Hobbs, H.C. Heard (Eds.), Mineral and Rock Deformation; Laboratory Studies; the Paterson volume, Am. Geophys. Union, Washington, DC, 1986, pp. 297–324.
[29] M. Herwegh, A new technique to automatically quantify microstructures of fine grained carbonate mylonites: two step etching combined with SEM imaging and image analysis, J. Struct. Geol. 22 (2000) 391–400.
[30] S.J. Covey-Crump, The normal grain growth behaviour of nominally pure calcitic aggregates, Contrib. Mineral. Petrol. 129 (1997) 239–254.
[31] D.L. Olgaard, B. Evans, Grain growth in synthetic marbles with added mica and water, Contrib. Mineral. Petrol. 100 (1988) 246–260.
[32] M. Herwegh, B. Evans, Grain growth and chemical exchange in polyphase rocks: Inferences from calcite-dolomite HIP experiments, EOS Trans. AGU 81 (2000) T12F-07.
[33] E.H. Rutter, The influence of temperature, strain rate and

interstitial water in the experimental deformation of calcite rocks, Tectonophysics 22 (1974) 311–334.
[34] J.R. Farver, R.A. Yund, Volume and grain boundary diffusion of calcium in natural and hot-pressed calcite aggregates, Contrib. Mineral. Petrol. 123 (1996) 77–91.
[35] J.R. Farver, R.A. Yund, Oxygen grain boundary diffusion in natural and hot-pressed calcite aggregates, Earth Planet. Sci. Lett. 161 (1998) 189–200.
[36] J.R. Farver, Oxygen self-diffusion in calcite: Dependence on temperature and water fugacity, Earth Planet. Sci. Lett. 121 (1994) 575–587.
[37] T.C. Labotka, D.R. Cole, L.R. Riciputi, Diffusion of C and O in calcite at 100 MPa, Am. Mineral. 85 (2000) 488–494.
[38] D.K. Fisler, R.T. Cygan, Diffusion of Ca and Mg in calcite, Am. Mineral. 84 (1999) 1392–1399.
[39] A.K. Kronenberg, R.A. Yund, B.J. Giletti, Carbon and oxygen diffusion in calcite: Effects of Mn content and P_{H2O}, Phys. Chem. Miner. 11 (1984) 101–112.
[40] D.L. Olgaard, B. Evans, Effect of second-phase particles on grain growth in calcite, J. Am. Ceram. Soc. 69 (1986) C272–C277.
[41] D.L. Olgaard, The role of second phase in localizing deformation, in: R.J. Knipe, E.H. Rutter (Eds.), Deformation Mechanisms, Rheology and Tectonics, Geol. Soc. Spec. Publ. 54 (1990) 175–181.
[42] M. Herwegh, A. Jenni, Granular flow in polymineralic rocks bearing sheet silicates new evidences from natural examples, Tectonophysics 332 (2001) 309–320.
[43] J. Newman, G. Mitra, Fluid-influenced deformation and recrystallization of dolomite at low temperature along a natural fault zone, Mountain City window, Tennessee, Geol. Soc. Am. Bull. 106 (1994) 1267–1280.
[44] D.V. Higgs, J.W. Handin, Experimental deformation of dolomite single crystals, Geol. Soc. Am. Bull. 70 (1959) 245–277.
[45] D.J. Barber, E.R.D. Scott, Transmission electron microscopy of carbonates and associated minerals in ALH 84001; impact induced deformation and carbonate decomposition, Meteorit. Planet. Sci. 36 (2001) 13–14.